J. Water Environ. Nanotechnol., 2(4): 265-277 Autumn 2017

ORIGINAL RESEARCH PAPER

Kinetic and Isotherm Studies of Cadmium Adsorption on Polypyrrole/Titanium dioxide Nanocomposite

Marjan Tanzifi[1,]*, Marzieh Kolbadi Nezhad[2], Kianoush Karimipour[1]

[1]Department of Chemical Engineering, Faculty of Engineering, University of Ilam, Ilam, Iran
[2]School of Chemical Gas and Petroleum Engineering, Semnan University, Semnan, Iran

Received: 2017-04-21 Accepted: 2017-05-22 Published: 2017-10-15

ABSTRACT
The present work seeks to investigate the ability of polypyrrole/titanium dioxide nanocomposite to adsorb cadmium ions from aqueous solution. The impact of various experimental conditions, including solution pH, adsorbent dosage, adsorption time and initial concentration on the uptake of cadmium were studied. The adsorption kinetic was studied with the first-order, second-order, pseudo-first-order, pseudo-second-order and Morris–Weber models. The results revealed that adsorption process is controlled by pseudo-second-order model which illustrated that the adsorption process of cadmium is chemisorption-controlled. The adsorption capacity obtained from this model is 20.49 mg/g which close to the experimental value. The study yielded the result that when the initial concentration of the solution changed from 20 mg/l to 120 mg/l, the adsorption capacity increased from 0.99 to 24.52 mg/g. Further, Langmuir, Freundlich and Temkin isotherm models were applied to investigate the adsorption isotherm. Based on the results of the adsorption isotherm, Freundlich isotherm proved to be the best fit with the experimental data. Also, the morphology, chemical structure and thermal stability of adsorbent were studied by using SEM, EDX, FTIR, and TGA.

Keywords: *Adsorption; Cadmium; Isotherm; Kinetic; Polypyrrole; Titanium Dioxide*

How to cite this article
Tanzifi M, Kolbadi Nezhad M, Karimipour K. Kinetic and Isotherm Studies of Cadmium Adsorption on Polypyrrole/Titanium dioxide Nanocomposite. J. Water Environ. Nanotechnol., 2017; 2(4): 265-277. DOI: 10.22090/jwent.2017.04.004

INTRODUCTION

Heavy metals due to be toxic and non-biodegradable are a serious threat to health and the environment. These metals are dissolved in water so can be transmitted by water and accumulate in soil and living organisms [1]. Among heavy metals, cadmium is a toxic one, which exists in natural, industrial and agricultural environments [2]. Exposure to cadmium can lead to the destruction of human organs (kidney, liver, and lung), immune system, and cardiovascular disease [3-5]. So, removal of cadmium from water is essential and necessary.

Various processes are presented for the removal of heavy metals from water and wastewater such as sedimentation, oxidation/reduction, membrane filtration, osmosis, ion exchange as well as adsorption. Among them, ion exchange/adsorption process is a convenient and economical way to produce high-quality water [6-8].

Today, nanotechnology is one of the most important trends in materials science. The term of nanotechnology refers to materials that one or more of their dimensions (length, width, and thickness) are in the range of nanometers (1-100 nm) [9]. Large specific surface, high reactivity and high adsorption and desorption capacity are main features of nanomaterials [9-12]. Due to these features, use of nanomaterials has increased in

* Corresponding Author Email: *m.tanzifi@ilam.ac.ir*

environmental applications [13,14]. Various nano-adsorbents such as Copper oxide nano blades [15], nanoscale zero-valent iron particles [16], CdS nanoparticles [17], nano magnetite/chitosan films [18] and nano zeolites [19] have been studied for the removal of cadmium.

Since the detection of conducting polymers, a lot of researches has been done in relation to the features and applications of these materials. Conductive polymers are used in different fields such as composite materials, biosensors as well as adsorption [20-22]. These materials have ion exchange capacity, which is dependent on conditions of polymerization and type of dopant and polymer [23]. Among the various conductive polymers, polypyrrole is considered due to its ease of polymerization, high chemical stability and biocompatibility [24-27]. Combination of polypyrrole with some materials can improve adsorption capacity. Ghorbani *et al* (2011), showed that polypyrrole is suitable adsorbent for removing zinc from aqueous solutions [28]. In a study conducted by John Chen *et al* (2015), polypyrrole/montmorillonite nanocomposite showed high adsorption capacity for the adsorption of chromium [29]. Mthombeni *et al* (2013), used magnetized natural zeolite-polypyrrole composite as a potential adsorbent for vanadium [30].

Titanium dioxide nanoparticles are used in catalysts [31], gas sensors [32], batteries [33] and environmental cleanup [34,35]. These particles, used as nano-fillers, lead to the modification of the polymeric network, which consequently, increases the surface area of the adsorbent. Fabrication of conductive polymer composites through titanium dioxide have been reported [36,37].

In this study, polypyrrole/titanium dioxide nanocomposite was considered as an effective nano-adsorbent for removing cadmium ions from aqueous solution. The impacts of four parameters, including adsorbent dosage, pH of the solution, adsorption time and initial concentration were scrutinized on the efficiency of cadmium adsorption. Also, kinetics and isotherms of cadmium adsorption on polypyrrole/titanium dioxide nanocomposite were studied.

EXPERIMENTAL

Materials and Instrumentation

In this study, pyrrole monomer, polyvinyl alcohol (PVA), ferric chloride (III) ($FeCl_3$), sulfuric acid, sodium hydroxide and cadmium salt purchased from Merck company of Germany and titanium dioxide nanoparticles (TiO_2) purchased from Kronos company of Germany. With the dissolution of $Cd(NO_3)_2.4H_2O$ in distilled water, 100 ppm cadmium solution was prepared. By using this solution, solutions with different concentrations were prepared. 1 M solution of sulfuric acid was used to change the pH. Pyrrole monomer was distilled for use in polymerization.

The equipment used in this research include: magnetic stirrer (model MK20), digital scale (model FR 200), Fourier transform infrared spectrometer (FTIR) (model VERTEX 70; BRUKER) and thermogravimetric analyzer (TGA) (model Perkin Elmer). Also, to describe the morphology of the polypyrrole/titanium dioxide and determine the concentration of cadmium ions in solution, the scanning electron microscope (SEM) (model XL30 and model KYKY-EM 3200) and atomic adsorption spectrophotometer (model Analytic Jena) were used, respectively. Atomic adsorption spectrophotometer calibrated using standard solutions (0.5-10 ppm) then the concentration of cadmium ions in each solution was measured.

Preparation of nano-adsorbent

In this method, 0.1 g of titanium dioxide nanoparticles was added to 50 ml of distilled water. Then 1 ml of pyrrole monomer and 0.3 g of polyvinyl alcohol as a stabilizer was added to the solution. After 30 minutes, a solution of ferric chloride as oxidant was added drop by drop to the above solution. By adding oxidant, the solution was initially green and then to black. This color change is a sign of conversion of pyrrole monomer to polypyrrole. Polymerization was carried out for 5 hours at ambient temperature. The polymer is then filtered. In order to remove oligomers and impurities, the polymer was washed several times with distilled water. The final product was dried for 48 hours in an oven at 45 °C. Then, the resulting polymer was milled to convert the powder. Also for comparison, pure polypyrrole and polypyrrole/titanium dioxide composite (without stabilizer) were synthesized [38].

Cadmium adsorption experiments

In the present study, the effects of different experimental conditions such as pH, initial concentration, adsorbent dose and adsorption time on removal of cadmium and also kinetic and isotherm results were studied. A Certain amount of

polypyrrole/titanium dioxide nanocomposite was added to 50 ml of cadmium solution with a certain initial concentration. Then, the solution was filtered and the concentration of cadmium ions was measured by atomic adsorption spectrophotometer. The adsorption efficiency is calculated by the following equation:

$$Removal(\%) = \frac{C_i - C_f}{C_i} \times 100 \quad (1)$$

In this equation, C_i and C_f represent the initial and final concentration of cadmium (mg/L), respectively. Also, q_e and q_t (mg/g) are adsorption capacity at equilibrium and time t, which calculated as follows:

$$q_e = (C_i - C_e) \times \frac{V}{m} \quad (2)$$

$$q_t = (C_i - C_t) \times \frac{V}{m} \quad (3)$$

Where Ce(mg/L) and C_t(mg/L) are the cadmium concentration at equilibrium and time t, respectively. Also, V is the volume of cadmium solution (L), and m is a mass of adsorbent (g).

RESULT AND DISCUSSION

Characterization of Adsorbent

Morphology of adsorbent was studied using scanning electron microscopy (SEM). Fig. 1 shows scanning electron microscope image of titanium dioxide nanoparticles. As can be seen, the particles have nearly spherical shape with an average diameter of 46 nm. Also, the particle size distribution is uniform. Fig. 2 shows SEM images of polypyrrole/titanium dioxide composite and polypyrrole/titanium dioxide nanocomposite made with polyvinyl alcohol. As can be seen in Fig. 2a, polypyrrole/titanium dioxide composite without stabilizer has large particle size. The morphology and particle size of products depend on the presence of stabilizer that reduces the size of the polymer particles. PVA affects on the physical and chemical features of the solution, the rate of formation of polypyrrole, morphology, homogenization, particle size and size distribution. The presence of PVA as a stabilizer in the polypyrrole/titanium dioxide synthesis media has several advantages. First, increase the solubility of the composite in aqueous solvents and then prevents the accumulation of particles in during polymerization. PVA is leading to a better quality of the final product [39]. As can be seen in Fig. 2b, by adding polyvinyl alcohol to the polypyrrole/titanium dioxide synthesis environment, smaller, spherical and uniform particles are produced, because polyvinyl alcohol affects the viscosity of the solution and polymerization rate. In fact, the use of stabilizer led to the formation of nano-adsorbent which has a positive effect on its performance in adsorption.

Fig. 3 shows the analysis of energy dispersive X-ray spectroscopy (EDX) of products. This

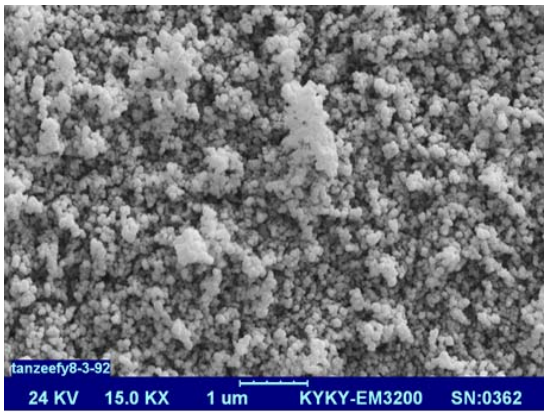

Fig. 1: Scanning electron micrograph of titanium dioxide nanoparticles.

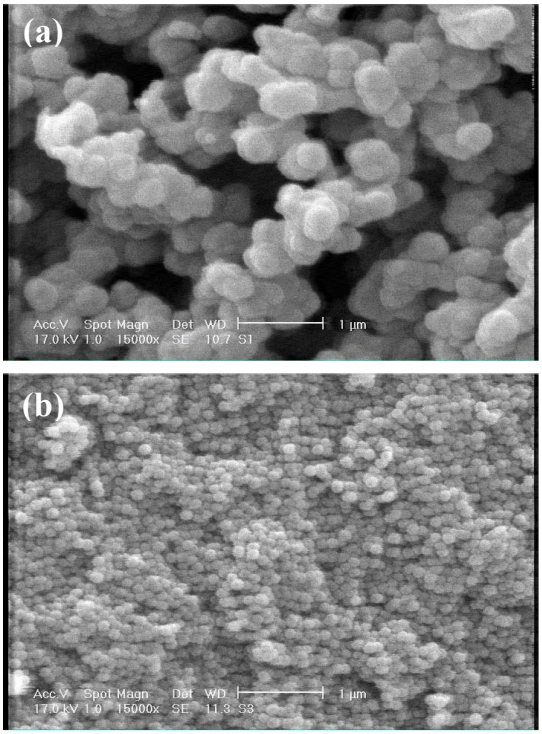

Fig. 2: Scanning electron micrograph of (a) polypyrrole/titanium dioxide composite and (b) polypyrrole/titanium dioxide nanocomposite (with PVA).

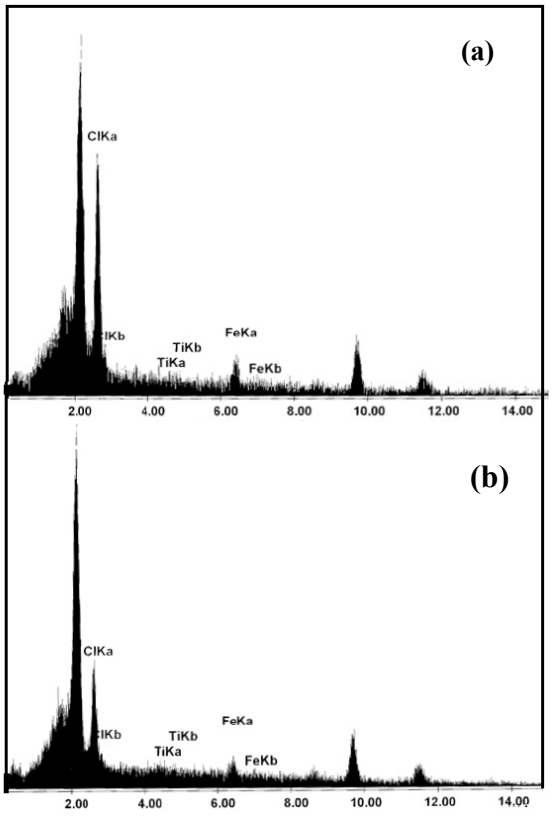

Fig.3: EDX analysis of (a) polypyrrole/titanium dioxide composite and (b) polypyrrole/titanium dioxide nanocomposite (with PVA).

analysis illustrates the presence of titanium dioxide nanoparticles in the synthesized nanocomposite. Further, Fe and Cl elements are related to ferric chloride (III), which was used as the oxidant. The presence of Fe and Cl ions in EDX spectrum shows that polypyrrole chain is doped by chloride anions. Table 1 presents the elemental compositions of synthesized polypyrrole/titanium dioxide composites with and without PVA which obtained from EDX analysis. Information obtained from SEM and EDX demonstrate the formation of polypyrrole in the presence of titanium dioxide nanoparticles.

The structure of synthesized products was specified by Fourier transform infrared (FTIR). Figs. 4a-4d are related to titanium dioxide nanoparticles, polypyrrole/titanium dioxide composite, pure polyvinyl alcohol and polypyrrole/titanium dioxide nanocomposite in presence of polyvinyl alcohol. The large peak at the wavelength 669 Cm^{-1} was ascribed to Ti-O bond (Fig. 4a). In Fig. 4b (FTIR spectra of polypyrrole/titanium dioxide composite), peak at 1547 Cm^{-1} is attributed to polypyrrole rings, which illustrates the polymer is generated. The other peaks are at 1313 cm^{-1} (C-N stretching vibration), 1175 cm^{-1} (C-H inplane deformation), 1043 cm^{-1} (N-H in-plane deformation), and 904 cm^{-1} (C-H out-of-plane deformation) [40]. The FTIR spectra of polypyrrole/titanium dioxide nanocomposite (Fig. 4d) shows all peaks of both PVA and polypyrrole nanocomposite have characteristic bands at 3457, 2973, 1844, 1533, 1445, 1293, 1159, 1039 cm^{-1} and 893 cm^{-1}, which are related to O-H band of PVA, C-H band of PVA, C=O band of PVA, pyrrole rings, CH_2 band of PVA, C-N band of polypyrrole, C-H band of polypyrrole, N-H group of polypyrrole and C-H band of polypyrrole, respectively. Also, a peak indicating the presence of titanium dioxide nanoparticles in the polymer can be seen in 667 Cm^{-1}. Results have been given in Table 2.

Table 1: EDX analysis data of polypyrrole/titanium dioxide with and without stabilizer

Sample	Elements (atoms%)		
	Fe	Ti	Cl
polypyrrole/titanium dioxide	41.31	6.81	51.88
polypyrrole/titanium dioxide (with PVA)	34.86	4.12	61.02

Table 2: FTIR spectra of polypyrrole/titanium dioxide with and without PVA

FTIR Spectra	Composite		
	Polypyrrole /titanium dioxide	Pure PVA	Polypyrrole /titanium dioxide (with PVA)
O-H	-	3392	3457
C-H	-	2941	2973
C=O	-	1717	1844
CH_2	-	1432	1445
C=C	1547	-	1533
C-N	1313	-	1293
C-H	1175	-	1159
N-H	1043	-	1039
C-H	904	-	893

In order to evaluate the impact of titanium dioxide nanoparticles on the thermal stability of polypyrrole, thermogravimetric analyzer (TGA) was used. Figs. 5a-5d illustrate TGA analysis of pure polypyrrole and its composite and nanocomposite. This analysis was performed under a nitrogen atmosphere in the temperature range 25-600 °C and the rate 10°C/min. TGA diagram of pure polypyrrole is shown in Fig. 5a. In this diagram, three stages of mass loss occur. The graph shows that mass loss begins at 30°C and continues until 140°C. The mass loss remains constant until 320°C and then fast mass loss happens from 320 to 600. At first, the mass loss causes by the elimination of water molecules to be in the polypyrrole structure and then increases by removing of oligomers. The next rapid mass loss can be related to the destruction of the polypyrrole chain. In Fig. 5c, removing the retained water in the polypyrrole network, which is ascribed to water molecules adsorbed due to the

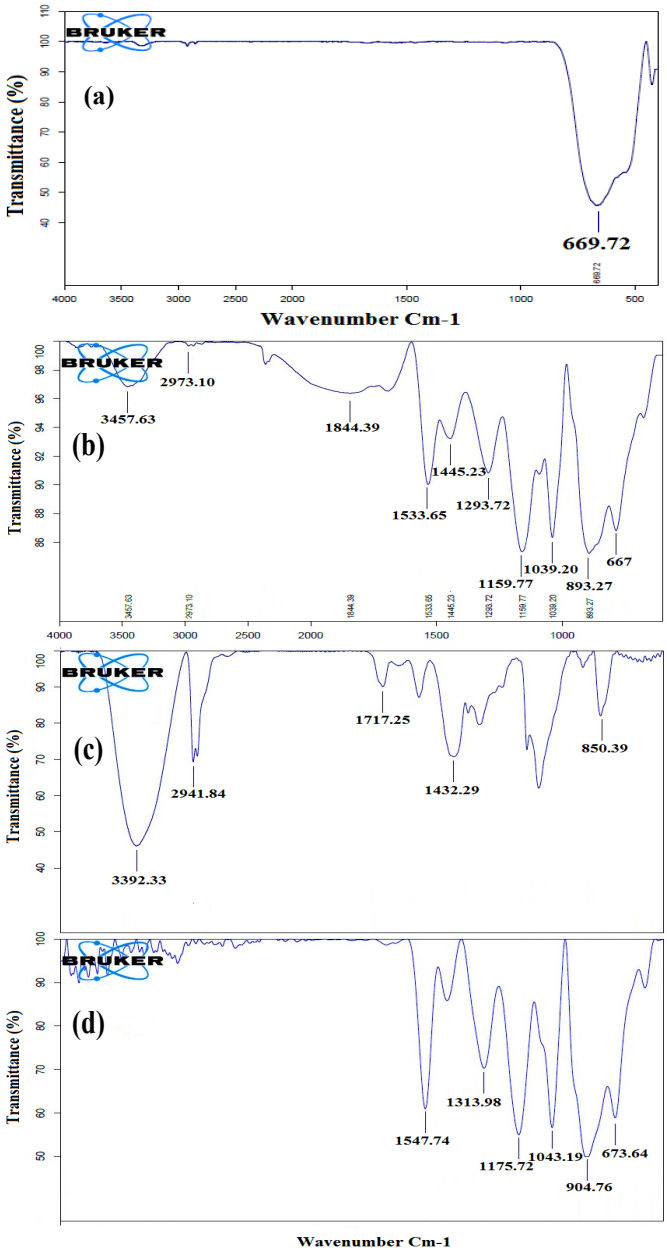

Fig. 4: FTIR spectra of (a) titanium dioxide nanoparticles (b) polypyrrole/titanium dioxide, (c) pure PVA and (d) polypyrrole/titanium dioxide (with PVA).

porous structure of polypyrrole [41], creates the first step of mass loss for the polypyrrole/titanium dioxide composite (about 7 wt% from 27°C to 148°C). The second mass loss stage (between 140°C to 380°C) has two reasons: The first reason is related to the loss of water molecules which form stronger bond with composite network and the second reason is related to the removal of volatile elements bound to polypyrrole chain and the omission of interaction between polypyrrole and titanium dioxide nanoparticles. Polypyrrole destruction and combustion at temperatures from 400-600°C, causes the third step on the mass loss. Mass loss in the temperature range 160-400°C (in Figs. 5b and 5d) can be ascribed to evaporation and degradation of polyvinyl alcohol. As can be seen, the thermal degradation rate of the nanocomposite, at temperatures above 350°C, is less than pure polypyrrole. Also according to Figs. 5a and 5d, mass loss of pure polypyrrole are 48% more than polypyrrole/titanium dioxide nanocomposite.

Effect of PH

The pH of the solution is an important parameter in the adsorption process of adsorbates. In this study, the effect of pH on adsorption efficiency of cadmium ions was investigated. The experiments were performed with the initial concentration of cadmium 50 mg/L, adsorption time 90 min and temperature 20°C. The experiments illustrated that at pH higher than 7 precipitate is formed (pH=7: sediment threshold). This shows that at the high pH, in addition of adsorption, deposit formation is also involved in the removal of cadmium. Therefore, cadmium uptake was studied in pH lower than 7. Results are shown in Fig. 6. As can be seen in the figure, in the range of pH=2.5 to 4.5, adsorption efficiency is maximum. By reducing the pH (less than 2.5), adsorption efficiency decreases. In low pH, the concentration of H^+ ions in the environment

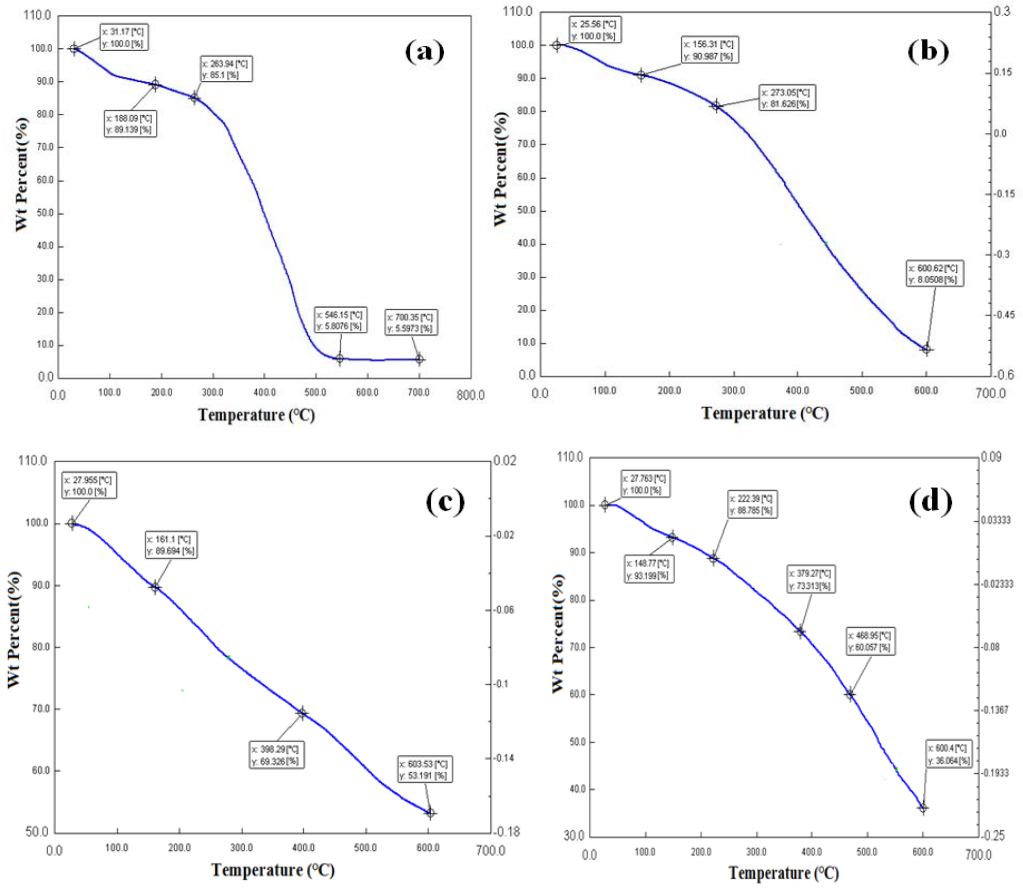

Fig. 5: TGA curve of (a) pure polypyrrole, (b) polypyrrole (with PVA), (c) polypyrrole/titanium dioxide and (d) polypyrrole/titanium dioxide (with PVA).

increases and these ions and metal ions compete on adsorption on the adsorbent surface, so the adsorption efficiency of metal ions is reduced. Polypyrrole/titanium dioxide nanocomposite has good performance in the range of pH=2.5-6.5, so it is suitable adsorbent in this pH range. Javadian and *et al*. showed that the effective adsorption of cadmium onto zeolite-based geopolymer occurs in the initial pH range of 2–5 [42].

Effect of amount of adsorbent

Adsorbent dosage is one of the important parameters in determining the adsorbed cadmium ions. In order to evaluate the impact of adsorbent dosage, varying amounts of polypyrrole/titanium dioxide nanocomposite (0.1 to 0.8 gr) were added to the 50 ml of cadmium solution (50 mg/l, pH=2.5). The effect of nanocomposite dosage on the uptake of cadmium is shown in Fig. 7. As can be seen, by increasing the amount of nanocomposite from 0.1 to 0.2 gr, cadmium adsorption efficiency increases from 60.26% to 67.76%, because of available adsorption places for a constant amount of cadmium increase. For higher adsorbent values, curves increase with a gentle slope, and this suggests that cadmium ions uptake efficiency increased slightly. The reason is that, by increasing the nanocomposite dosage, nanomaterials due to a large specific surface and high reactivity, stick together and form a lump. So, adsorption efficiency does not change much. The optimum adsorbent dosage was considered 0.2 g.

Effect of initial concentration and cadmium adsorption Isotherm

Solutions with an initial concentration of 20-

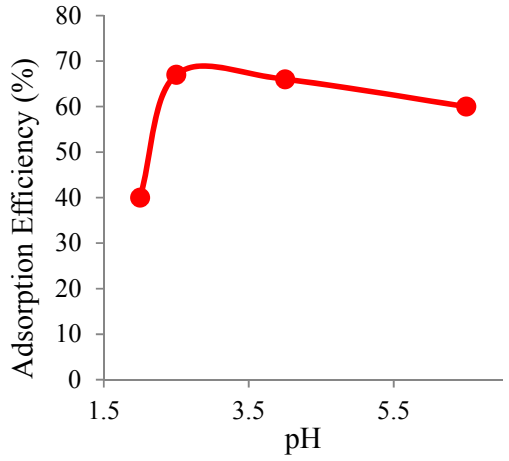

Fig. 6: Effect of pH on the adsorption efficiency of cadmium.

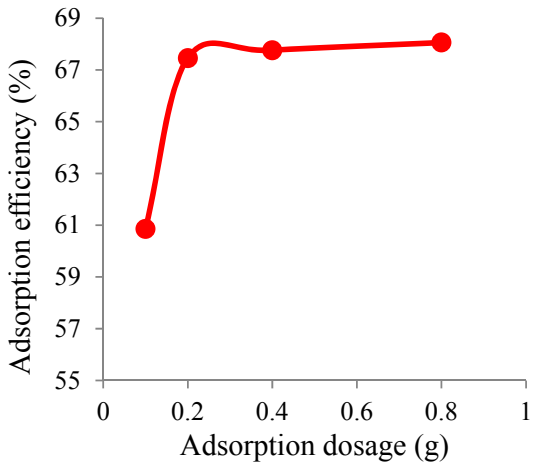

Fig. 7: Effect of adsorbent dosage on the adsorption efficiency of cadmium.

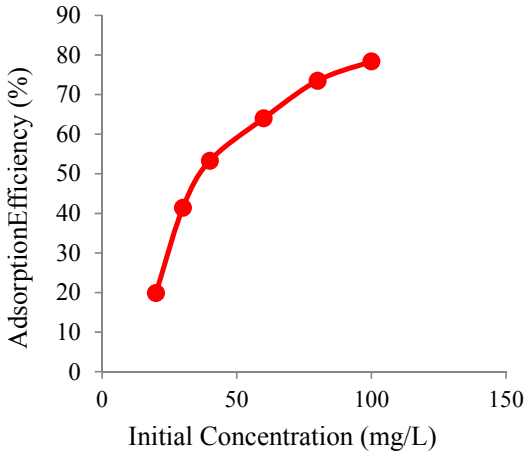

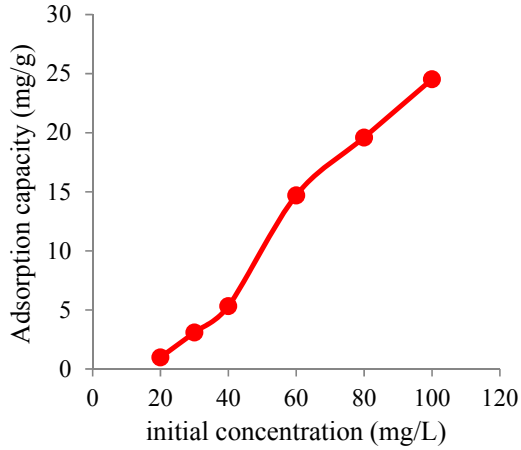

Fig. 8: Effect of initial concentration on the adsorption efficiency and capacity.

120 ppm, was prepared to investigate the impact of initial concentration of cadmium ions on adsorption efficiency and capacity. Nanocomposite dosage, PH, adsorption time and volume solution were considered 0.2 g, 2.5, 90 min and 50 ml, respectively. As shown in Fig. 8, the adsorption efficiency and capacity increase with increasing initial concentration of cadmium ions. When initial concentration increases from 20 to 120 mg/L, adsorption efficiency and capacity change from 19.9 to 81.74% and 0.995 to 24.52 mg/g, respectively.

Adsorption isotherm models illustrate the relationship between the cadmium concentration in solution and the quantity of cadmium ions adsorbed onto the specified amount of nanocomposite at a steady temperature. In this study, three adsorption isotherm models, namely; Langmuir, Freundlich, and Temkin were investigated.

In the Langmuir isotherm model, the adsorption energy is independent of surface coverage. All adsorption places are similar to each other and each place can adsorb only one type. This model is expressed by the following equation [43]:

$$q_e = \frac{q_m K_L C_e}{1 + K_L C_e} \quad (4)$$

where q_e, C_e and q_m are the quantity of adsorbed cadmium for the specified amount of nanocomposite (mg/g), equilibrium cadmium concentration (mg/L) and maximum adsorption capacity of nanocomposite (mg/g), respectively. Also, K_L is Langmuir constant. The Linear form of this equation presented as:

$$\frac{C_e}{q_e} = \frac{1}{q_m K_L} + \frac{1}{q_m} C_e \quad (5)$$

Separation factor (R_L) is a dimensionless constant that represents the essential specifications of the Langmuir isotherm:

$$R_L = \frac{1}{1 + K_L c_i} \quad (6)$$

where Ci is the initial concentration of cadmium solution and K_L is Langmuir constant. As the R_L obtained between 0-1, cadmium adsorption process onto nanocomposite is *favorable*. Langmuir plot is shown in Fig. 9. The negative slope of curve demonstrated that Langmuir equation is not appropriate for this data [28].

Freundlich model is an empiric equation that applied for adsorption on heterogeneous surfaces which is expressed as follows [44]:

$$q_e = K_F (C_e)^{1/n} \quad (7)$$

This equation can be written in linear form as follow:

$$log(q_e) = log(K_F) + \frac{1}{n} log(c_e) \quad (8)$$

K_f and 1/n are Freundlich constant and adsorption intensity, respectively, which calculated from intercept and slope of plot of $log(q_e)$ versus $log(C_e)$. Freundlich model plot is shown in Fig. 10. Temkin Isotherm has a factor that reflects interactions between adsorbate particles (cadmium) and adsorbent (nanocomposite). The equation of the isotherm can be expressed as follows [45]:

$$q_e = \frac{RT}{b_T} \ln(K_T C_e) \quad (9)$$

The above equation can be expressed in linear form as follows:

$$q_e = B \ln(K_T) + B ln\,(C_e) \quad (10)$$

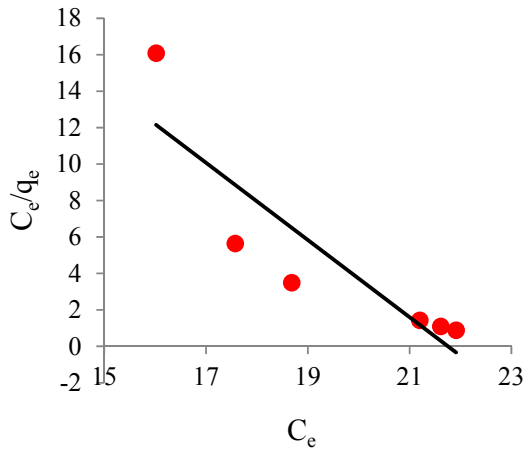

Fig. 9: Langmuir adsorption isotherm of cadmium ions onto polypyrrole/titanium dioxide nanocomposite.

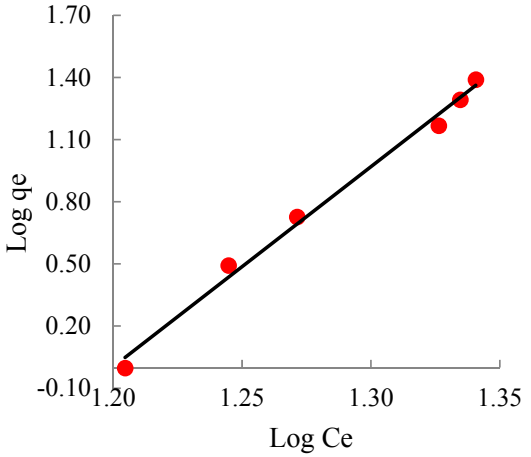

Fig. 10: Freundlich adsorption isotherm of cadmium ions onto polypyrrole/titanium dioxide nanocomposite.

$$B = \frac{RT}{b_T} \quad (11)$$

Where K_T, B, R, T, and b_T are equilibrium binding constant of Temkin (L/g), Temkin isotherm constant, universal gas constant (8.314 J/mol.K), absolute temperature (298.15 K) and constant appertained to adsorption heat (J/mol), respectively. Fig. 11 shows the Temkin isotherm plot.

The constants and correlation coefficient (R^2) for all isotherm models are illustrated in Table 3. Results show that Freundlich isotherm is the best model that represents the behavior of cadmium adsorption process onto polypyrrole/titanium dioxide nanocomposite because this model offers the highest correlation coefficient compared to other isotherms.

Effect of adsorption time and cadmium adsorption kinetics

Fig. 12 illustrates the effect of adsorption time on the adsorption of cadmium ions onto polypyrrole/titanium dioxide nanocomposite. The initial concentration of cadmium and pH were considered 100 ppm and 2.5. Also, adsorbent dosage was 0.2 g per 50 ml of cadmium solution. The impact of adsorption time on cadmium adsorption efficiency was conducted with the change in time from 2 to 100 min. The results showed that with increasing adsorption time, adsorption efficiency of cadmium increased. Adsorption efficiency reached from 78.4% to 82.01% with increasing the time from 2 to 100 min. As can be seen, removal of cadmium by polypyrrole/titanium dioxide nanocomposite, reached 81.8% at adsorption time 5 min. This demonstrated that in the short time, a large amount of cadmium is adsorbed by the polypyrrole/titanium dioxide nano-adsorbent.

Different kinetic models including the first-order, second-order, pseudo-first-order, pseudo-second and Morris–Weber were used to investigate the cadmium adsorption onto polypyrrole/titanium dioxide nanocomposite adsorbent. Kinetic models explain the adsorption rate of cadmium ions and it is clear that it controls the adsorption time in the intersection of the solution and solid.

The first-order equation is expressed in the linear form as follows:

$$\ln\left(\frac{C_0}{C_t}\right) = K_1 t \quad (12)$$

Where C_0, C_t, and K_1 are initial concentration, cadmium concentration at time t and rate constant of the first-order model. Fig. 13 shows $\ln\left(\frac{C_0}{C_t}\right)$ versus *t* plot.

Table 3: Isotherm parameters for cadmium adsorption

Isotherm	parameters
Langmuir	y = -2.1186x+46.092 R^2 = 0.7817 R_L: (−2.63) − (−0.278) K = 2.6×10^{-12}
Freundlich	n = 0.103 R^2 = 0.9925 B= 70.77
Temkin	K_T = 0.699 R^2 = 0.887

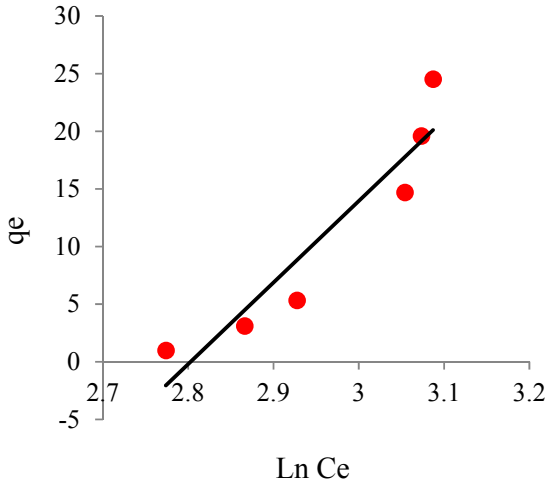

Fig. 11: Temkin adsorption isotherm of cadmium ions onto polypyrrole/titanium dioxide nanocomposite.

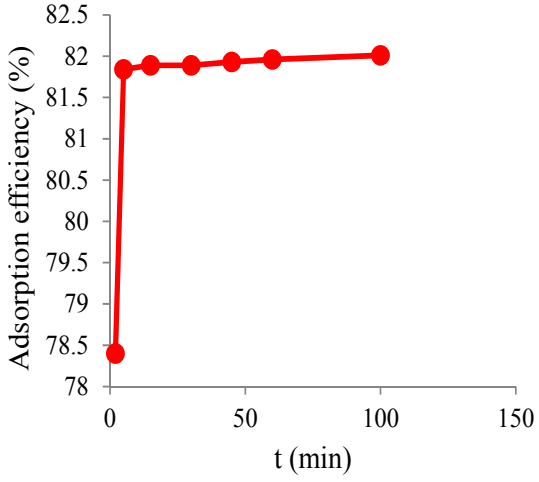

Fig. 12: Effect of adsorption time on adsorption efficiency.

The linear form of the second-order model is presented as follows:

$$\frac{1}{C_t} = K_2 t + \frac{1}{C_0} \quad (13)$$

where K_2 is rate constant of the second-order model which gained from slop of $\frac{1}{C_t} - \frac{1}{C_0}$ versus plot (Fig. 14).

In 1898, lagergren [46] presented the pseudo-first-order kinetic model for solid/liquid adsorption system based on adsorbent capacity. It presumes that the variation rate of adsorbate removal with time is straightly proportional to the difference in the saturation concentration and the quantity of solid adsorption with time. Pseudo-first-order equation is expressed as follows:

$$log(q_e - q_t) = log q_e - \left(\frac{K}{2.303}\right) t \quad (14)$$

where q_e and q_t are cadmium adsorption capacity at equilibrium and at time t. K is a constant rate of pseudo-first-order model. Fig. 15 shows the pseudo-first-order plot for adsorption cadmium adsorbed onto polypyrrole/titanium dioxide nanocomposite.

Kinetic data of cadmium adsorption onto polypyrrole/titanium dioxide nanocomposite were also investigated by the pseudo-second-order equation. This kinetic model assumes that cadmium adsorption process is chemisorption. It is presented as follow [47]:

$$q_t = \frac{K q_e{}^2 t}{1 + K q_e t} \quad (15)$$

The linear form of this equation can express as:

$$\frac{t}{qt} = \frac{1}{K_2 qe^2} + \frac{1}{qe} t \quad (16)$$

where K_2 is the equilibrium rate constant of pseudo-second-order model (g/mg.min). The values of parameters of this model and regression coefficient (R^2) are summarized in Table 4. As shown in Fig. 16, $\frac{t}{qt}$ versus plot was a direct line with slope $\frac{1}{qe}$ and intercept $\frac{1}{K_2 qe^2}$.

Morris-Weber model illustrates that the intra-particle diffusion is a stage of speed controller

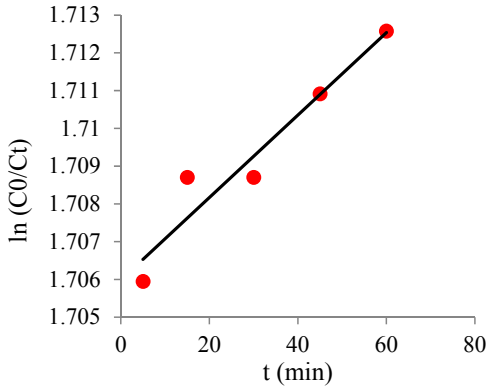

Fig. 13: First-order plot of cadmium adsorption onto polypyrrole/titanium dioxide nanocomposite.

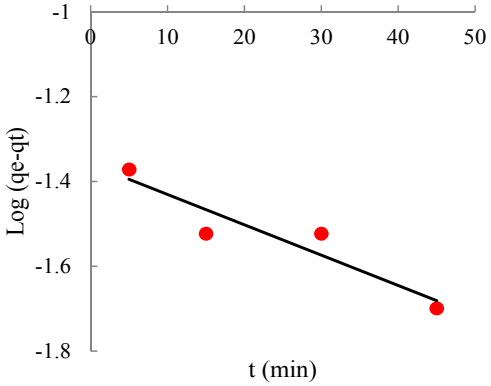

Fig. 15: Pseudo-first-order plot of cadmium adsorption onto polypyrrole/titanium dioxide nanocomposite.

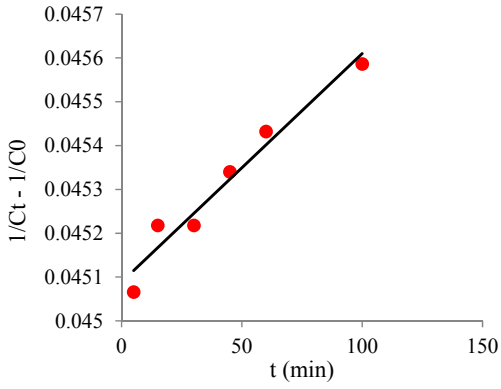

Fig. 14: Second-order plot of cadmium adsorption onto polypyrrole/titanium dioxide nanocomposite.

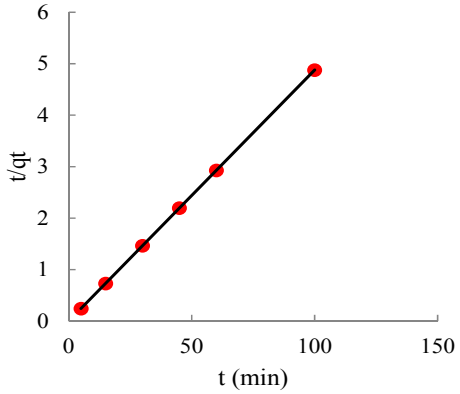

Fig. 16: Pseudo-second-order plot of cadmium adsorption onto polypyrrole/titanium dioxide nanocomposite.

in adsorption process [48]. This equation was expressed as follows:

$$q_t = K_{id}(t)^{0.5} + C \quad (17)$$

In this equation, K_{id} is rate constant of intra-particle diffusion and C is a parameter depended on boundary layer thickness. If the Morris-Weber plot is linear, the process of cadmium adsorption is controlled by diffusion resistance. When the line passes through the origin, it indicates that intra-particle diffusion is the only rate-controlling step. The plot of qt versus $t^{0.5}$ is shown in Fig. 17. K_{id} and C constants are calculated from the slope and intercept of this plot.

Information gained from five kinetic equations is presented in Table 4. The correlation coefficient for first-order, second-order, pseudo-first-order, pseudo-second-order and Morris-Weber models were obtained 0.9279, 0.9554, 0.8765, 1 and 0.9641, respectively. As a result, cadmium adsorption process was controlled by pseudo-second-order model, which demonstrated that adsorption of cadmium onto polypyrrole/titanium dioxide nanocomposite is a chemical adsorption process. In studies conducted by Yang *et al* (2015) and Javadian *et al* (2016), adsorption of cadmium onto zeolite and carbon/aluminum composite were also controlled by pseudo-second-order kinetic model [41,49].

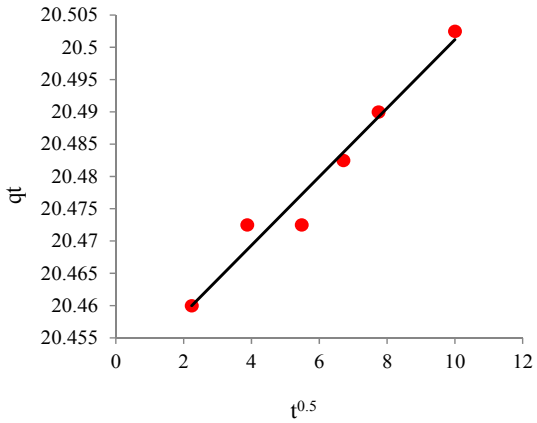

Fig. 17: Morris-Weber plot of cadmium adsorption onto polypyrrole/titanium dioxide nanocomposite

Table 4: Kinetic parameters for cadmium adsorption

Kinetic model	parameters
First-order	K_1=0.0001 R^2 =0.9279
Second-order	K_2=5×10^{-6} R^2 =0.9554
pseudo-first-order	q_e (experimental) =19.59 q_e (calculated) =22.85 K =0.016 R^2 = 0.8765
pseudo-second-order	q_e (experimental) =19.59 q_e (calculated) =20.4918 K =1.4884 R^2 = 1
Morris-Weber	K_{id} =0.0053 C= 20.448 R^2 =0.9641

CONCLUSION

In this research, polypyrrole/titanium dioxide nanocomposite was prepared using polymerization of pyrrole monomer in the presence of ferric chloride (III) oxidant and stabilizer of polyvinyl alcohol at an ambient temperature and applied as a cadmium adsorbent from the water. Polypyrrole/titanium dioxide nanocomposite with the nano-sized particles has a high adsorption efficiency. The optimized conditions for adsorption cadmium were achieved adsorbent dosage 0.2 gr, pH 2.5 and adsorption time 60 min. Adsorption data matched well with the Freundlich model. The research yielded the result that cadmium adsorption process was controlled by pseudo-second-order model which demonstrates the chemical adsorption. Also, the adsorption capacity of nanocomposite obtained from this model was 20.49 mg/g, which is close to the empirical value. In addition, adsorbent characteristics such as thermal stability, chemical structure, and morphology were studied. EDX Analysis proved the presence of titanium dioxide nanoparticles in the nanocomposite structure. Also, the chemical structure of the synthesized nanocomposite was analyzed by FTIR. TGA results illustrated that the produced composite and nanocomposite of polypyrrole showed considerable thermal stability compared to pure polypyrrole.

CONFLICT OF INTEREST

The authors declare that there are no conflicts of interest regarding the publication of this manuscript.

REFERENCES

1. Kurniawan TA, Chan GYS, Lo W-H, Babel S. Physico–chemical treatment techniques for wastewater laden with heavy metals. CHEM ENG J. 2006;118(1):83-98.
2. Järup L. Hazards of heavy metal contamination. BRIT MED BULL. 2003;68(1):167-82.
3. Fowler BA. Monitoring of human populations for early markers of cadmium toxicity: A review. Toxicol Appl Pharmacol. 2009;238(3):294-300.
4. Järup L, Åkesson A. Current status of cadmium as an

environmental health problem. Toxicol Appl Pharmacol. 2009;238(3):201-8.
5. Thompson J, Bannigan J. Cadmium: Toxic effects on the reproductive system and the embryo. Reprod Toxicol. 2008;25(3):304-15.
6. Ghiloufi I, Ghoul JE, Modwi A, Mir LE. Ga-doped ZnO for adsorption of heavy metals from aqueous solution. Mater Sci Semicond Process. 2016;42(Part 1):102-6.
7. Liao B, Sun W-y, Guo N, Ding S-l, Su S-j. Equilibriums and kinetics studies for adsorption of Ni(II) ion on chitosan and its triethylenetetramine derivative. Colloids Surf, A. 2016;501(Supplement C):32-41.
8. Zareie C, Najafpour G. Preparation of nanochitosan as an effective sorbent for the removal of copper ions from aqueous solutions. International Journal of Engineering-Transactions B: Applications. 2013;26(8):829-36.
9. Tian J, Xu J, Zhu F, Lu T, Su C, Ouyang G. Application of nanomaterials in sample preparation. J Chromatogr A. 2013;1300(Supplement C):2-16.
10. El-Nahhal IM, Zourab SM, Kodeh FS, Elmanama AA, Selmane M, Genois I, et al. Nano-structured zinc oxide–cotton fibers: synthesis, characterization and applications. Journal of Materials Science: Materials in Electronics. 2013;24(10):3970-5.
11. Yan XM, Shi BY, Lu JJ, Feng CH, Wang DS, Tang HX. Adsorption and desorption of atrazine on carbon nanotubes. J Colloid Interface Sci. 2008;321(1):30-8.
12. Yusan S, Korzhynbayeva K, Aytas S, Tazhibayeva S, Musabekov K. Preparation and investigation of structural properties of magnetic diatomite nanocomposites formed with different iron content. J Alloys Compd. 2014;608(Supplement C):8-13.
13. Teimouri A, Nasab SG, Vahdatpoor N, Habibollahi S, Salavati H, Chermahini AN. Chitosan /Zeolite Y/Nano ZrO2 nanocomposite as an adsorbent for the removal of nitrate from the aqueous solution. Int J Biol Macromol. 2016;93(Part A):254-66.
14. Shojaei S, Khammarnia S, Shojaei S, Sasani M. Removal of Reactive Red 198 by Nanoparticle Zero Valent Iron in the Presence of Hydrogen Peroxide. Journal of Water and Environmental Nanotechnology. 2017;2(2):129-35.
15. Bhanjana G, Dilbaghi N, Singhal NK, Kim K-H, Kumar S. Copper oxide nanoblades as novel adsorbent material for cadmium removal. Ceram Int. 2017;43(8):6075-81.
16. Azzam AM, El-Wakeel ST, Mostafa BB, El-Shahat MF. Removal of Pb, Cd, Cu and Ni from aqueous solution using nano scale zero valent iron particles. J Environ Chem Eng. 2016;4(2):2196-206.
17. Raj R, Dalei K, Chakraborty J, Das S. Extracellular polymeric substances of a marine bacterium mediated synthesis of CdS nanoparticles for removal of cadmium from aqueous solution. J Colloid Interface Sci. 2016;462(Supplement C):166-75.
18. Lasheen MR, El-Sherif IY, Tawfik ME, El-Wakeel ST, El-Shahat MF. Preparation and adsorption properties of nano magnetite chitosan films for heavy metal ions from aqueous solution. Mater Res Bull. 2016;80(Supplement C):344-50.
19. Yousefi T, Torab-Mostaedi M, Charkhi A, Aghaei A. Cd(II) Sorption on Iranian nano zeolites: Kinetic and Thermodynamic Studies. Journal of Water and Environmental Nanotechnology. 2016;1(2):75-83.
20. Zuo X, Zhang Y, Si L, Zhou B, Zhao B, Zhu L, et al. One-step electrochemical preparation of sulfonated graphene/polypyrrole composite and its application to supercapacitor. J Alloys Compd. 2016;688(Part B):140-8.
21. Tanzifi M, Mansouri M, Heidarzadeh M, Gheibi K. Study of the Adsorption of Amido Black 10B Dye from Aqueous Solution Using Polyaniline Nano-adsorbent: Kinetic and Isotherm Studies. Journal of Water and Environmental Nanotechnology. 2016;1(2):124-34.
22. Tanzifi M, Karimipour K, Najafifard M, Mirchenari S. REMOVAL OF CONGO RED ANIONIC DYE FROM AQUEOUS SOLUTION USING POLYANILINE/TIO2 AND POLYPYRROLE/TIO2 NANOCOMPOSITES: ISOTHERM, KINETIC, AND THERMODYNAMIC STUDIES. International Journal of Engineering-Transactions C: Aspects. 2016;29(12):1659.
23. Weidlich C, Mangold KM, Jüttner K. Conducting polymers as ion-exchangers for water purification. Electrochim Acta. 2001;47(5):741-5.
24. Waltman RJ, Bargon J. Reactivity/structure correlations for the electropolymerization of pyrrole: An INDO/CNDO study of the reactive sites of oligomeric radical cations. TETRAHEDRON. 1984;40(20):3963-70.
25. Waltman RJ, Bargon J. Electrically conducting polymers: a review of the electropolymerization reaction, of the effects of chemical structure on polymer film properties, and of applications towards technology. Can J Chem. 1986;64(1):76-95.
26. Ruckenstein E, Chen J-H. Polypyrrole conductive composites prepared by coprecipitation. POLYMER. 1991;32(7):1230-5.
27. Diaz A. Electrochemical preparation and characterization of conducting polymers. CHEM SCRIPTA. 1981;17(1-5):145-8.
28. Omraei M, Esfandian H, Katal R, Ghorbani M. Study of the removal of Zn(II) from aqueous solution using polypyrrole nanocomposite. DESALINATION. 2011;271(1):248-56.
29. Chen J, Hong X, Xie Q, Tian M, Li K, Zhang Q. Exfoliated polypyrrole/montmorillonite nanocomposite with flake-like structure for Cr(VI) removal from aqueous solution. Res Chem Intermed. 2015;41(12):9655-71.
30. Mthombeni NH, Mbakop S, Ochieng A, Onyango MS. Vanadium (V) adsorption isotherms and kinetics using polypyrrole coated magnetized natural zeolite. J Taiwan Inst Chem Eng. 2016;66(Supplement C):172-80.
31. Zhong S, Ou Q, Shao L. PHOSPHORUS PROMOTED SO4 (2-)/TiO2 SOLID ACID CATALYST FOR ACETALIZATION REACTION. J Chil Chem Soc. 2015;60(3):3005-6.
32. Alev O, Şennik E, Kılınç N, Öztürk ZZ. Gas Sensor Application of Hydrothermally Growth TiO2 Nanorods. Procedia Eng. 2015;120(Supplement C):1162-5.
33. Kashale AA, Gattu KP, Ghule K, Ingole VH, Dhanayat S, Sharma R, et al. Biomediated green synthesis of TiO2 nanoparticles for lithium ion battery application. Composites Part B: Engineering. 2016;99(Supplement C):297-304.
34. Niehues E, Scarminio IS, TAKASHIMA K. Optimization of photocatalytic decolorization of the azo dye direct orange 34 by statistical experimental design. J Chil Chem Soc. 2010;55(3):320-4.
35. Kamal T, Anwar Y, Khan SB, Chani MTS, Asiri AM. Dye adsorption and bactericidal properties of TiO2/chitosan coating layer. Carbohydr Polym. 2016;148(Supplement C):153-60.
36. Gao F, Hou X, Wang A, Chu G, Wu W, Chen J, et al. Preparation of polypyrrole/TiO2 nanocomposites with enhanced photocatalytic performance. Particuology. 2016;26(Supplement C):73-8.
37. Zou Y, Wang Q, Jiang D, Xiang C, Chu H, Qiu S, et al. Pd-doped TiO2@polypyrrole core-shell composites as hydrogen-sensing materials. Ceram Int. 2016;42(7):8257-62.

38. Eisazadeh H, Ghorbani M. Copolymerization of pyrrole and vinyl acetate in aqueous and aqueous/nonaqueous media. J Vinyl Add Tech. 2009;15(3):204-10.
39. Rinaldi AW, Kunita MH, Santos MJL, Radovanovic E, Rubira AF, Girotto EM. Solid phase photopolymerization of pyrrole in poly(vinylchloride) matrix. Eur Polym J. 2005;41(11):2711-7.
40. Ghorbani M, Eisazadeh H. Fixed bed column study for Zn, Cu, Fe and Mn removal from wastewater using nanometer size polypyrrole coated on rice husk ash. Synth Met. 2012;162(15):1429-33.
41. Zhang H, Li GR, An LP, Yan TY, Gao XP, Zhu HY. Electrochemical Lithium Storage of Titanate and Titania Nanotubes and Nanorods. The Journal of Physical Chemistry C. 2007;111(16):6143-8.
42. Javadian H, Ghorbani F, Tayebi H-a, Asl SH. Study of the adsorption of Cd (II) from aqueous solution using zeolite-based geopolymer, synthesized from coal fly ash; kinetic, isotherm and thermodynamic studies. Arabian J Chem. 2015;8(6):837-49.
43. Langmuir I. The constitution and fundamental properties of solids and liquids. J Franklin Inst. 1917;183(1):102-5.
44. Freundlich H. Over the adsorption in solution. J Phys Chem. 1906;57(385471):1100-7.
45. Temkin M, Pyzhev V. Kinetics of ammonia synthesis on promoted iron catalysts. Acta physiochim URSS. 1940;12(3):217-22.
46. Lagergren S. About the theory of so-called adsorption of soluble substances. KUNGLIGA SVENSKA VETENSKAPSAKADEMIENS HANDLINGAR. 1898;24(4):1-39.
47. Ho YS, McKay G. Pseudo-second order model for sorption processes. Process Biochem. 1999;34(5):451-65.
48. Weber WJ, Morris JC. Kinetics of adsorption on carbon from solution. Journal of the Sanitary Engineering Division. 1963;89(2):31-60.
49. Yang W, Tang Q, Wei J, Ran Y, Chai L, Wang H. Enhanced removal of Cd(II) and Pb(II) by composites of mesoporous carbon stabilized alumina. Appl Surf Sci. 2016;369(Supplement C):215-23.